Electronic Supplementary Material (ESI) for Dalton Transactions

Supporting Information

for

Electronic Tuning of Nitric Oxide Release from Manganese Nitrosyl Complexes by Visible Light Irradiation: Enhancement of Nitric Oxide Release Efficiency by Nitro-Substituted Quinoline Ligand

Yutaka Hitomi*, Yuji Iwamoto, Masahito Kodera

Department of Molecular Chemistry and Biochemistry, Faculty of Science and Engineering, Doshisha University, 1-3 Tatara Miyakodani, Kyotanabe, 610-0321 Kyoto, Japan

yhitomi@mail.doshisha.ac.jp

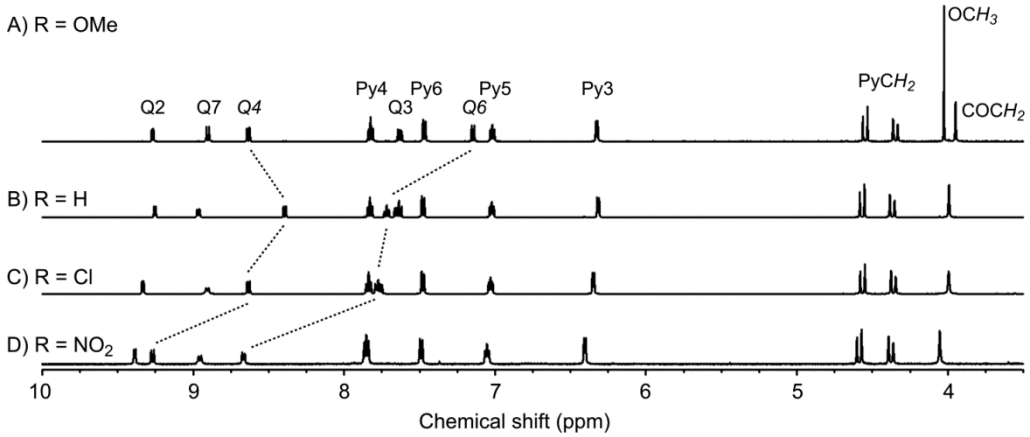

Fig. S1 ^{1}H NMR spectra of $\mathbf{1}^{\mathbf{OMe}}$ (A), $\mathbf{1}^{\mathbf{H}}$ (B), $\mathbf{1}^{\mathbf{Cl}}$ (C) and $\mathbf{1}^{\mathbf{NO2}}$ (D) in CD_3CN.

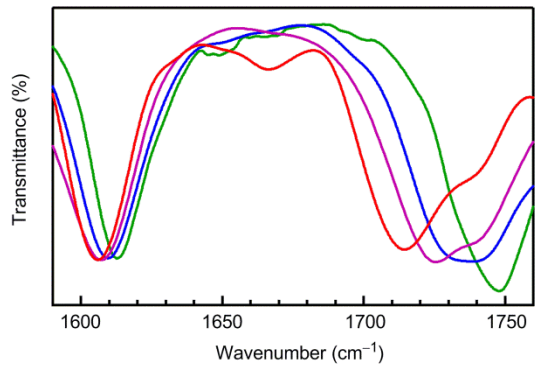

Fig. S2 ATR-IR spectra of $\mathbf{1}^{\mathbf{R}}$ (R: OMe, green; H, blue; Cl, purple and NO_2, red).

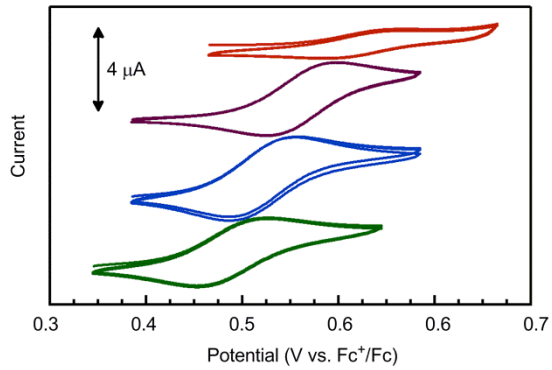

Fig. S3 Cyclic voltamogram of $\mathbf{1}^{\mathbf{R}}$ (R: OMe, green; H, blue; Cl, purple and NO_2, red) in deaerated CH_3CN containing 0.1 M *n*-Bu_4NClO_4 at 25°C; working electrode Pt, counter electrode Pt, reference electrode Ag/AgCl in CH_3CN, scan rate 20 mV s^{-1}. $E_{1/2}$ (*vs.* Fc^+/Fc (ΔE)): 0.49 V (75 mV) for R = OMe; 0.52 V (71 mV) for R = H; 0.56 V (73 mV) for R = Cl and 0.63 V (81 mV) for R = NO_2.

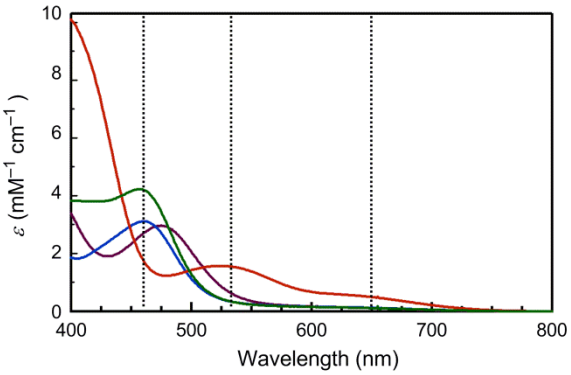

Fig. S4 Electric absorption spectra of $\mathbf{1}^{\mathbf{R}}$ (R: OMe, green; H, blue; Cl, purple and NO_2, red) in MES buffer (pH 7.2) at 20 °C. Vertical dotted lines show the wavelengths of light irradiation (460, 530 and 650 nm).

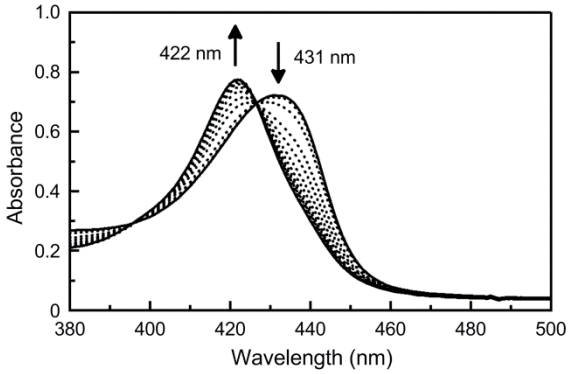

Fig. S5 Conversion of reduced myoglobin (ca. 1.7 μM, λ_{max} = 431 nm) to the NO adduct of myoglobin (λ_{max} = 422 nm) by the photolysis of $\mathbf{1}^{\mathbf{NO2}}$ (20 μM) in MES buffer (pH 7.2) under N_2.

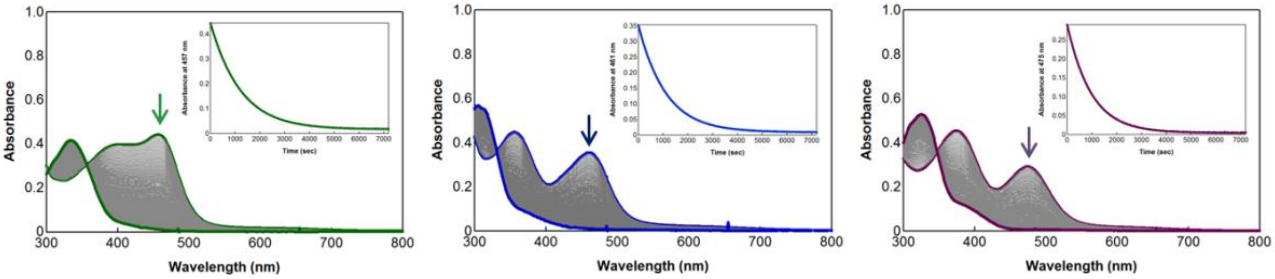

Fig. S6 Electronic spectral change of solutions of $\mathbf{1}^{\mathbf{OMe}}$ (left), $\mathbf{1}^{\mathbf{H}}$ (middle) and $\mathbf{1}^{\mathbf{Cl}}$ (right) in MES buffer (pH 7.2, 5% DMSO) at 20 °C under irradiation at 650 nm. The arrows indicate a decrease in band intensities as the reaction proceeds. Inset: Time profiles of the absorbance at 457 nm for $\mathbf{1}^{\mathbf{OMe}}$, 461 nm for $\mathbf{1}^{\mathbf{H}}$ and 475 nm for $\mathbf{1}^{\mathbf{Cl}}$.

Table S1. Summary of Crystal Data and Intensity Collection and Structural Refinement Parameters for $\mathbf{1}^{R}$ Derivatives.

	$\mathbf{1}^{OMe}$	$\mathbf{1}^{H}$	$\mathbf{1}^{Cl}$	$\mathbf{1}^{NO2}$
Empirical formula	$C_{24}H_{22}ClMnN_6O_7$	$C_{23}H_{20}ClMnN_6O_6$	$C_{23}H_{19}Cl_2MnN_6O_6$	$C_{25}H_{22}ClMnN_8O_8$
Formula weight	596.87	566.84	601.28	652.90
Crystal color and habit	brown platelet	brown block	brown platelet	brown chip
Crystal size (nm)	0.29 × 0.19 × 0.10	0.30 × 0.10 × 0.10	0.08 × 0.05 × 0.03	0.30 × 0.10 × 0.10
Temperature (K)	133	133	133	133
Crystal system	triclinic	monoclinic	monoclinic	monoclinic
Space group	*P*-1	$P2_1/n$	$P2_1/c$	*Pc*
a (Å)	8.6256(5)	12.3007(5)	8.88120(10)	8.50240(10)
b (Å)	11.7224(9)	13.3626(6)	10.14710(10)	7.29870(10)
c (Å)	13.1577(10)	14.1948(7)	26.2914(5)	21.7032(5)
α (°)	71.050(4)	90	90	90
β (°)	87.566(4)	107.070(2)	92.9655(8)	98.8707(11)
γ (°)	80.591(3)	90	90	90
Volume ($Å^3$)	1241.30(15)	2230.41(17)	2366.17(6)	1330.71(4)
Z	2	4	4	2
D_{calc} (Mg/m^3)	1.597	1.688	1.688	1.642
Absorption coefficient, μ (mm^{-1})	5.829	6.417	7.104	5.549
Reflections collected	16650	28188	31658	10774
Independent reflections [R_{int}]	2542 [0.1127]	2237 [0.1213]	2634 [0.0515]	2990 [0.0777]
Max. and min. transmission	0.5933 and 0.2827	0.5660 and 0.2489	0.8151 and 0.6003	0.6068 and 0.2868
Goodness-of-fit on F^2	1.126	1.090	1.057	1.031
Final *R* indices [$I>2\sigma(I)$]	$R_1 = 0.0752$, $wR_2 = 0.1902$	$R_1 = 0.1080$, $wR_2 = 0.2588$	$R_1 = 0.0346$, $wR_2 = 0.0766$	$R_1 = 0.0522$, $wR_2 = 0.1136$
R indices (all data)	$R_1 = 0.0969$, $wR_2 = 0.2268$	$R_1 = 0.1479$, $wR_2 = 0.3130$	$R_1 = 0.0424$, $wR_2 = 0.0809$	$R_1 = 0.0599$, $wR_2 = 0.1229$

Table S2. Selected Bond Lengths (Å) and Angles (deg) for $\mathbf{1}^{R}$ Derivatives

	$\mathbf{1}^{OMe}$	$\mathbf{1}^{H}$	$\mathbf{1}^{Cl}$	$\mathbf{1}^{NO2}$
Mn(1)-N(1)	2.000(7)	2.036(11)	2.008(3)	2.024(5)
Mn(1)-N(2)	2.028(7)	2.121(9)	2.044(3)	2.075(6)
Mn(1)-N(3)	2.063(6)	2.120(10)	2.068(3)	2.061(5)
Mn(1)-N(4)	1.923(7)	1.998(9)	1.941(3)	1.957(5)
Mn(1)-N(5)	2.015(6)	2.129(9)	2.038(3)	2.052(5)
Mn(1)-N(6)	1.742(8)	1.635(12)	1.713(4)	1.660(5)
N(6)-O(2)	1.015(7)	1.022(16)	1.044(4)	1.136(7)
C(20)-O(1)	1.247(9)	1.225(15)	1.240(4)	1.217(7)
O(2)-N(6)-Mn(1)	176.7(8)	171(2)	171.3(3)	175.8(6)
N(6)-Mn(1)-N(4)	177.0(3)	176.9(6)	173.37(13)	176.4(2)
N(6)-Mn(1)-N(1)	96.0(3)	98.1(7)	94.74(13)	96.6(2)
N(4)-Mn(1)-N(1)	81.3(3)	78.9(5)	80.50(12)	80.1(2)
N(6)-Mn(1)-N(5)	99.3(3)	100.7(6)	101.98(13)	99.5(2)
N(4)-Mn(1)-N(5)	83.4(3)	82.3(4)	82.87(11)	83.8(2)
N(1)-Mn(1)-N(5)	164.7(3)	161.0(4)	163.26(12)	163.72(18)
N(6)-Mn(1)-N(2)	92.7(3)	92.3(6)	93.81(13)	95.2(2)
N(4)-Mn(1)-N(2)	86.6(2)	87.4(3)	91.45(11)	86.7(2)
N(1)-Mn(1)-N(2)	99.3(3)	96.7(4)	98.15(12)	101.4(2)
N(5)-Mn(1)-N(2)	81.0(3)	80.1(4)	80.32(12)	79.9(2)
N(6)-Mn(1)-N(3)	94.7(3)	90.4(6)	91.57(13)	93.5(2)
N(4)-Mn(1)-N(3)	86.8(2)	91.0(3)	84.60(11)	85.6(2)
N(1)-Mn(1)-N(3)	97.0(3)	104.3(4)	98.37(12)	95.6(2)
N(5)-Mn(1)-N(3)	80.8(3)	78.2(4)	81.89(12)	80.8(2)
N(2)-Mn(1)-N(3)	161.3(3)	158.2(5)	162.12(12)	159.9(2)

Table S3. ^{1}H NMR Signal Assignment of $\mathbf{1}^{R}$ Derivatives

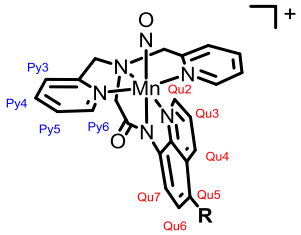

	$\mathbf{1}^{OMe}$	$\mathbf{1}^{H}$	$\mathbf{1}^{Cl}$	$\mathbf{1}^{NO2}$
Py3	6.33 (d, 2H, *J* = 5.2 Hz)	6.31 (d, 2H, *J* = 5.7 Hz)	6.35 (d, 2H, *J* = 5.2 Hz)	6.41 (d, 2H, *J* = 5.2 Hz)
Py4	7.82 (t, 2H, *J* = 7.7 Hz)	7.83 (t, 2H, *J* = 7.7 Hz)	7.84 (t, 2H, *J* = 7.7 Hz)	7.85 (m, 3H)
Py5	7.02 (t, 2H, *J* = 6.6 Hz)	7.02 (t, 2H, *J* = 6.6 Hz)	7.03 (t, 2H, *J* = 6.6 Hz)	7.05 (t, 2H, *J* = 6.3 Hz)
Py6	7.47 (d, 2H, *J* = 8.0 Hz)	7.48 (d, 2H, *J* = 8.0 Hz)	7.48 (d, 2H, *J* = 8.0 Hz)	7.46 (d, 2H, *J* = 8.0 Hz)
Qu2	9.27 (dd, 1H, *J* = 1.7, 5.2 Hz)	9.25 (d, 1H, *J* = 5.2 Hz)	9.33 (d, 1H, *J* = 5.0 Hz)	9.39 (d, 1H, *J*= 5.2 Hz)
Qu3	7.63 (dd, 1H, *J* = 5.1, 8.5 Hz)	7.65 (dd, 1H, *J* = 5.1, 8.3 Hz)	7.77 (m, 2H??)	7.85 (m, 3H???)
Qu4	8.63 (dd, 1H, *J* = 8.6, 1.2 Hz)	8.39 (d, 1H, *J* = 8.6 Hz)	8.63 (d, 1H, *J* = 8.6 Hz)	9.27 (d, 1H, *J* = 8.6 Hz)
Qu5	–	7.63 (d, 1H, *J* = 8.0 Hz)	–	–
Qu6	7.15 (d, 1H, *J* = 8.6 Hz)	7.72 (t, 1H, *J* = 8.0, 8.0 Hz)	7.77 (m, 2H)	8.67 (d, 1H, *J* = 8.6 Hz)
Qu7	8.90 (d, 1H, *J* = 8.6 Hz)	8.97 (d, 1H, *J* = 8.0 Hz)	8.92 (d, 1H, *J* = 8.6 Hz)	8.96 (d, 1H, *J* = 8.6 Hz)
-CH_2CO-	3.95 (s, 2H)	4.00 (s, 2H)	3.99 (s, 2H)	4.05 (s, 2H)
PyCH_2-	4.55 (d, 2H, *J* = 15.5 Hz)	4.57 (d, 2H, *J* = 15.5 Hz)	4.56 (d, 2H, *J* = 15.5 Hz)	4.59 (d, 2H, *J* = 15.5 Hz)
PyCH_2-	4.35 (d, 2H, *J* = 15,5 Hz)	4.37 (d, 2H, *J* = 15.5 Hz)	4.36 (d, 2H, *J* = 15.5 Hz)	4.38 (d, 2H, *J* = 15.5 Hz)
OCH_3	4.03 (s, 3H)	–	–	–

Table S5. Electronic Absorption Bands of Ligands and Complexes[a]

	H-dpaq^{R} in CH_3CN	[Mn^{II}(dpaq^{R})]ClO_4 in CH_3CN	**1^{R}** in CH_3CN	**1^{R}** in MES buffer (pH 7.2)
R = OMe	346 (4740), 252 (38700)	405 (3320), 346 (2330), 264 (33200)	459 (5090), 356 (2450), 265 (25300)	457 (4230), 398 (3830)
R = H	320 (5780), 244 (40800)	375 (4500), 262 (37100)	459 (3940), 382 (4160), 259 (25900)	461 (3120), 357 (3910)
R = Cl	333 (6940), 246 (34300)	388 (5330), 264 (25900)	474 (3760), 398 (5140), 260 (26900)	475 (2960), 375 (4560)
R = NO_2	368 (13600), 241 (24400)	428 (19100), 322 (3990), 262 (22900)	513 (2070), 423 (14500), 314 (5870), 264 (20600)	523 (1570), 392 (10300)

[a] Molar extinction coefficient ($M^{-1}cm^{-1}$) in parentheses.

Table S6. Initial Rate Constant of the Decomposition of {MnNO}^{6} Complexes Under Light Irradiation

complex	k_{int} ($\mu M\ s^{-1}$)		
	460 nm	530 nm	650 nm
1^{OMe}	1.71 ± 0.05	0.254 ± 0.004	0.0835 ± 0.0009
1^{H}	1.79 ± 0.02	0.300 ± 0.005	0.0999 ± 0.0018
1^{Cl}	1.26 ± 0.13	0.494 ± 0.013	0.0988 ± 0.010
1^{NO2}	0.84 ± 0.05	0.809 ± 0.017	0.395 ± 0.006
2	2.94 ± 0.11	0.203 ± 0.006	0.252 ± 0.004